SIAM J. APPL. MATH.
Vol. 61, No. 5, pp. 1526–1544

SOME PROPERTIES OF GENERALIZED AGE-DISTRIBUTION EQUATIONS IN FLUID DYNAMICS*

J. M. BECKERS†, E. DELHEZ‡, AND E. DELEERSNIJDER§

Abstract. The concept of age in fluid dynamics is analyzed in the case of a tracer advection-diffusion equation. From the general solution in a uniform velocity field, it is shown that unexpected symmetry properties arise for the age field. In particular, for a point release, the age field is isotropic, regardless of the direction of the flow and the value of the diffusion coefficient. The analysis is then extended to situations with time-varying currents, where the symmetry can be broken under some circumstances. Finally, we show a method by which a time-dependent problem can be used to assess a stationary concentration distribution function, providing details about the propagation of younger and older material at a given location.

Key words. age, advection diffusion

AMS subject classifications. 76R05, 76R50, 35Q35

PII. S0036139999363810

1. Introduction.

In natural physical systems, both experimental measurements and complex mathematical models usually yield such huge amounts of data that the underlying processes may become extremely difficult to understand. By using appropriate diagnostic tools, tractable information about the system may be easily extracted. In the case of natural flows, age provides such a diagnostic tool.

The age of a water parcel is usually defined as "the time elapsed since the parcel under consideration left the region in which its age is defined to be zero" (e.g., [30, 26, 10]). Such a region can be defined in various ways so that the actual definition of age can be made to suit any specific focus on the flow's intrinsic time scales.

The concept of age is widely used in ocean sciences to assess time scales associated with the ventilation of the deep ocean controlled by vertical advection and diffusion processes (e.g., [27, 5, 25, 13, 17, 19, 6]). In this case, the age is taken to be zero at the surface. The age of a water parcel located in the core of the ocean thus indicates the time elapsed since that parcel was last exposed to the surface. It is therefore a summary of the complex history of such a water parcel and helps to understand the ventilation of the deep ocean.

In shelf seas, age can be used to follow the spreading of coastal water, river plumes, or pollutant patches using both natural and artificial tracers released from both point sources and distributed sources (e.g., [20, 23, 24, 2, 28, 11]).

For instance, radioactive tracers released at the nuclear fuel reprocessing plants of La Hague (English Channel) and Sellafield (Irish Sea) have been used to quantify the transit time from these locations to any point in the North Sea (e.g., [22, 23]). In this case, the age is taken to be zero at the source point so that the age of a parcel of the studied tracer at any other location is representative of the time scales associated with the transport from the source to this location.

*Received by the editors October 29, 1999; accepted for publication (in revised form) August 16, 2000; published electronically January 19, 2001. This work was supported by the National Fund for Scientific Research, Belgium.

http://www.siam.org/journals/siap/61-5/36381.html

†University of Liège, Sart-Tilman B5, B-4000 Liège, Belgium (JM.Beckers@ulg.ac.be).

‡University of Liège, Sart-Tilman B37, B-4000 Liège, Belgium (E.Delhez@ulg.ac.be).

§Université Catholique de Louvain-La-Neuve, Unité ASTR, Chemin du cyclotron, B-1348 Louvain-La-Neuve, Belgium (ericd@astr.ucl.ac.be).

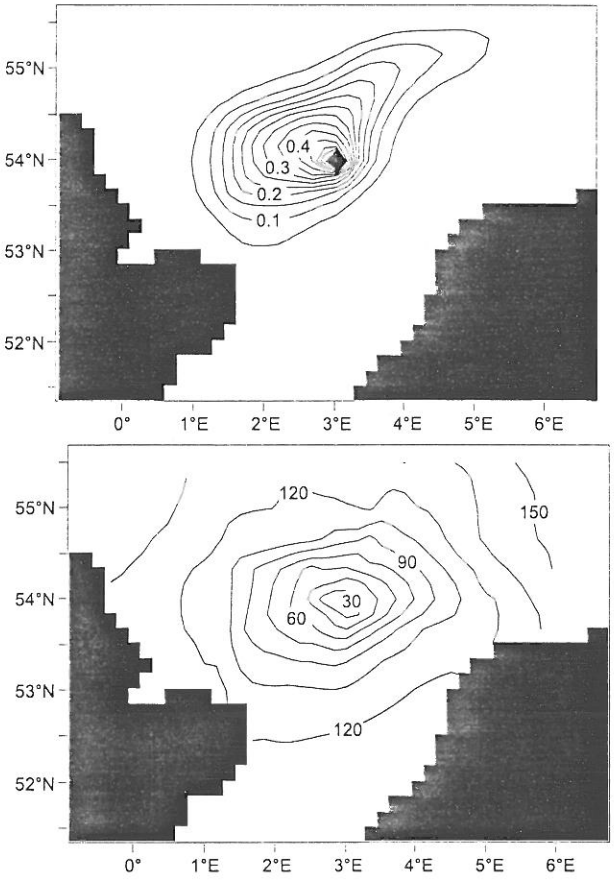

FIG. 1. *Concentration (normalized) and age field (in days) for passive tracer release experiment in the North Sea.*

Insofar as the age can be both computed with numerical models and assessed experimentally using radioactive dating techniques and oxygen or CFC data analysis, it can also be used to compare, calibrate, and validate ocean circulation models (e.g., [4, 13, 23, 15, 8, 9]).

The previous examples introduce only a limited number of successful applications of the age theory. If this theory is to provide a better insight into complex flows, one must have a thorough understanding of the dynamics of age itself. It is therefore the aim of this paper to explore some of the characteristics of age dynamics.

In particular, part of this work is motivated by one of the surprising results obtained in the scope of the NOMADS project. In the framework of this concerted action, five numerical models of the North Sea were compared with respect to, among other aspects, the age field associated with the release of a passive tracer in the center of the North Sea [1].

Figure 1 shows the resulting concentration and age fields computed by the GHER model [9]. All the models (with various spatial resolutions and numerical characteristics) considered in this model intercomparison experiment exhibited similar results. The concentration field shows an elongated patch reflecting the particular circulation pattern at the time of the simulation (winter 1988 to spring 1989). While preferential

direction of spreading of the patch can be clearly identified in the concentration field, no such direction appears in the age field, suggesting a quasi-isotropic propagation of age! This counterintuitive result is one of the points studied in the following sections.

2. Elements of the theory of age. A general theory of the age concept has been recently proposed by [10, 7]. This theory takes into account advection, diffusion, production, and destruction processes of scalar tracers. It can be shown that most of the forms previously suggested in the literature may be deduced from this general theory after certain simplifications and hypotheses [7]. This theory thus provides a theoretical framework in which the different aspects of the dynamics of age can be studied in detail.

This approach also overcomes (see [10]) the problem associated with the poor account of the diffusion process in previous age studies (e.g., [18, 21, 27, 29, 19]).

Following [10, 7], we introduce the concept of a concentration distribution function $c(t, \boldsymbol{x}, \tau)$ depending on time t, space $\boldsymbol{x}$, and age τ. c is the concentration of material whose age equals τ. As shown in [10], the concentration distribution function $c(t, \boldsymbol{x}, \tau)$ satisfies a generalized advection-diffusion equation ($\boldsymbol{u}$ is the velocity field, $\boldsymbol{K}$ the diffusion tensor, $\boldsymbol{\nabla} = \sum_i \boldsymbol{e}_i \frac{\partial}{\partial x_i}$ the Nabla operator, and $p - d$ source and sink terms of material of age τ)

$$\frac{\partial c}{\partial t} = p - d - \boldsymbol{\nabla} \cdot (\boldsymbol{u} c - \boldsymbol{K} \cdot \boldsymbol{\nabla} c) - \frac{\partial c}{\partial \tau}. \tag{2.1}$$

The standard tracer concentration $C(t, \boldsymbol{x})$ can be calculated as

$$C(t, \boldsymbol{x}) = \int_0^\infty c(t, \boldsymbol{x}, \tau) \, \mathrm{d}\tau \tag{2.2}$$

and leads to the classical advection-diffusion equation for a tracer:

$$\frac{\partial C}{\partial t} = P - D - \boldsymbol{\nabla} \cdot (\boldsymbol{u} C - \boldsymbol{K} \cdot \boldsymbol{\nabla} C) \tag{2.3}$$

with

$$P = c(\boldsymbol{x}, \tau = 0) - c(\boldsymbol{x}, \tau = \infty) + \int_0^\infty p \, \mathrm{d}\tau, \quad D = \int_0^\infty d \, \mathrm{d}\tau \tag{2.4}$$

being the total source and sink terms of the tracer.

In addition, the average age, i.e., the mean age of the tracer, is defined as the mass weighted age [10, 7]:

$$a(t, \boldsymbol{x}) = \frac{1}{C} \int_0^\infty \tau c(t, \boldsymbol{x}, \tau) \, \mathrm{d}\tau. \tag{2.5}$$

From here on, when no confusion is possible, a (the mean age) will be referred to as "age."

If one is not interested in calculating the age distribution function c, based on (2.1) one may calculate the age a by solving an advection-diffusion equation for the so-called age-concentration field $\alpha = aC$ satisfying

$$\frac{\partial \alpha}{\partial t} = \pi - \delta + C - \boldsymbol{\nabla} \cdot (\boldsymbol{u} \alpha - \boldsymbol{K} \cdot \boldsymbol{\nabla} \alpha), \tag{2.6}$$

$$\pi = \int_0^\infty \tau p \, d\tau, \quad \delta = \int_0^\infty \tau d \, d\tau. \tag{2.7}$$

Once the age-concentration α is known, the mean age can be retrieved from $a = \frac{\alpha}{C}$. Another approach is to write down explicitly the partial differential equation governing the field a by using the differential equations for C and α, which leads to the following equation (for a symmetric diffusion tensor $\boldsymbol{K}$):

$$\frac{\partial a}{\partial t} = 1 + \frac{\pi - aP}{C} - \frac{\delta - aD}{C} - \boldsymbol{\nabla}\cdot(u a - \boldsymbol{K}\cdot\boldsymbol{\nabla} a) + 2\frac{\boldsymbol{\nabla} C\cdot \boldsymbol{K}\cdot \boldsymbol{\nabla} a}{C}. \tag{2.8}$$

This equation is useful for theoretical understanding. From a practical point of view, in numerical models, (2.3) and (2.6) are solved more easily than (2.8). This is due to the fact that the latter is of a different type compared to the other two, which are easily treated by standard numerical solvers of advection-diffusion equations (see [10, 7] for a discussion).

In this formulation of the age theory, the distinction can be made among the age of a single tracer, the age of an aggregate of tracers, and that of the water itself. This makes it possible to study the fate of tracers, like CFC or oxygen (e.g., [29, 3, 19]), of the radioactive tracers, like tritium, carbon-14 (e.g., [12, 17, 6]), or of the water. The age of the water itself is in fact merely the age of a tracer with a unit concentration. In this case, the previous equations are reduced (see [10]) to an expression equivalent to the one used by [15] and [13]. It is further possible to define an artificial tracer marking a given water mass and to follow its transport and spreading through the system (e.g., [16]).

3. Some properties and general solutions. It is worth noting that the equations allow the superposition of solutions for the concentration C and the age concentration α but not the age a.

If, for example, one has a tracer with a linear external source term $P - D = Q_1$ with a prescribed age of zero, giving rise to the solution C_1 and α_1 and another tracer with a source term $P - D = Q_2$ with solution C_2 and α_2, it is easy to verify that the solution to the problem for adequate boundary conditions with a source $Q_1 + Q_2$ is $C = C_1 + C_2$, $\alpha = \alpha_1 + \alpha_2$. For age, however, the solution is not a simple superposition but reads $(C_1 + C_2)a = C_1 a_1 + C_2 a_2$.

In the following section, we will focus on a still relatively general case of the preceding concepts by analyzing the case of a tracer with radioactive-like decay in a constant current field $\boldsymbol{u}$[1] with isotropic diffusion $\boldsymbol{K} = \kappa \boldsymbol{I}$ and a source term which is a combination of an external supply Q and linear decay with a decay rate of $1/T$. The results will thus be applicable to natural radioactive or conservative (setting $1/T \to 0$) tracers, or to artificial (numerical) tracers used to flag specific water masses. Classically, for radioactive tracers, one looks at their evolution from the moment they have been injected into the system, so that for the external source the age-concentration is prescribed to be zero.

In this case, the equations can be rendered nondimensional by defining

$$\tilde{t} = \frac{t}{4\kappa\|u\|^{-2}}, \ \tilde{x} = \frac{x}{4\kappa\|u\|^{-1}}, \ v = \frac{u}{\|u\|}, \ \tilde{\alpha} = \frac{\alpha}{4\kappa\|u\|^{-2}}, \ \gamma = \frac{4\kappa}{T\|u\|^2}, \ \tilde{a} = \frac{a}{4\kappa\|u\|^{-2}} \tag{3.1}$$

[1]The analysis will be extended later to a case where $\boldsymbol{u} = \boldsymbol{u}(t)$, requiring scaling by means of a typical velocity scale so that $v(t) = O(1)$.

so that for a source term q (omitting the $\tilde{}$) the nondimensional equations read

$$\frac{\partial C}{\partial t} = q - \gamma C - \boldsymbol{v}\cdot\nabla C + \frac{1}{4}\nabla^2 C, \tag{3.2}$$

$$\frac{\partial \alpha}{\partial t} = C - \gamma\alpha - \boldsymbol{v}\cdot\nabla\alpha + \frac{1}{4}\nabla^2\alpha, \tag{3.3}$$

$$\frac{\partial a}{\partial t} = 1 - \frac{q}{C}a - \left(\boldsymbol{v} - \frac{\nabla C}{2C}\right)\cdot\nabla a + \frac{1}{4}\nabla^2 a. \tag{3.4}$$

We introduced a nondimensional form of the equations for the sake of clearer mathematical presentation, but we do not have to assume that the nondimensional equations are balanced, since our scaling is arbitrary. The diffusion term can be completely negligible or dominant depending on the value of the diffusion coefficient and the velocity scale. Our analysis will thus be valid for advection-dominated flows, diffusion-dominated flows, or mixed situations. Furthermore, the decay rate can also take any value, so that the analysis is valid for tracers which decay very rapidly within the flow or, on the contrary, are conserved for a long time. Strictly conservative tracers are of course obtained for $\gamma = 0$. When presenting the results, we generally maintain the nondimensional forms, but one has to bear in mind that the dimensional form will show the dependence on velocity and on the diffusion scale.

So far, uniformity of current was not a necessary assumption, since the nondimensional velocity vector $\boldsymbol{v}$ could be variable in space and time. When examining a flow field locally (in time and space), the flow can, however, be considered locally to be uniform. In this case, we can establish certain properties which are likely to exist in real situations in regions where the flow is relatively uniform—a not uncommon situation.

A simple solution for such uniform-flow equations can be found for a Dirac point release $q(\boldsymbol{x},t) = Q\delta(\boldsymbol{x})\delta(t)$ in $t = 0$ into a system with zero concentration at the initial moment:

$$C(\boldsymbol{x},t) = \frac{Q}{\sqrt{\pi t}^n}\exp\left[\frac{-(\boldsymbol{x}-\boldsymbol{v}t)^2}{t}\right]\exp(-\gamma t), \tag{3.5}$$

$$\alpha(\boldsymbol{x},t) = t\frac{Q}{\sqrt{\pi t}^n}\exp\left[\frac{-(\boldsymbol{x}-\boldsymbol{v}t)^2}{t}\right]\exp(-\gamma t), \tag{3.6}$$

where $n = 1$ for a one-dimensional (1D) problem, $n = 2$ for a two-dimensional (2D) problem, and $n = 3$ for a point release in three-dimensional (3D) problems.

Of course, for such a release, the age α/C is simply $a = t$ everywhere, since the tracer was injected only at the beginning with zero age. For 1D, 2D, and 3D cases, it is easily verified that total tracer mass is $q\exp[-\gamma t]$ reflecting the decay and the initial mass injected into the system.

From the basic solution of an instantaneous point release, one can derive the solution in an infinite domain for any type of release (regardless of the solution) by using the classical convolution theorem which is merely the superposition of individual contributions from the Dirac solutions. In other words, we can use the Green function to calculate the general solution:

$$C(\boldsymbol{x},t) = \int_{R^n}\int_0^t \frac{q(\boldsymbol{x}',t')}{\sqrt{\pi(t-t')}^n} e^{\left[\frac{-(\boldsymbol{x}-\boldsymbol{x}'-\boldsymbol{v}(t-t'))^2}{t-t'} - \gamma(t-t')\right]} \mathrm{d}t'\mathrm{d}\boldsymbol{x}', \tag{3.7}$$

$$\alpha(\boldsymbol{x},t)=\int_{R^n}\int_0^t \frac{(t-t')q(\boldsymbol{x}',t')}{\sqrt{\pi(t-t')}^n} e^{\left[\frac{-(\boldsymbol{x}-\boldsymbol{x}'-\boldsymbol{v}(t-t'))^2}{t-t'}-\gamma(t-t')\right]}\mathrm{d}t'\mathrm{d}\boldsymbol{x}', \tag{3.8}$$

from which the age can then be retrieved as $a=\alpha/C$.

One can verify that if the source is independent of a coordinate in a direction perpendicular to the velocity vector, the solution may be integrated along this direction, thus reducing the terms of the problem from R^n to R^{n-1}.

3.1. Point release. For a point release ($q(\boldsymbol{x},t)=\delta(\boldsymbol{x})Q(t)$) the integrals (3.7) and (3.8) simplify to

$$C(\boldsymbol{x},t)=\int_0^t \frac{Q(t-t')}{\sqrt{\pi t'}^n}\exp\left[\frac{-(\boldsymbol{x}-\boldsymbol{v}t')^2}{t'}\right]\exp\left[-\gamma t'\right]\mathrm{d}t', \tag{3.9}$$

$$\alpha(\boldsymbol{x},t)=\int_0^t \frac{t'Q(t-t')}{\sqrt{\pi t'}^n}\exp\left[\frac{-(\boldsymbol{x}-\boldsymbol{v}t')^2}{t'}\right]\exp\left[-\gamma t'\right]\mathrm{d}t'. \tag{3.10}$$

By observing that $(\boldsymbol{x}-\boldsymbol{v}t)^2/t=-2\boldsymbol{x}\cdot\boldsymbol{v}+\|\boldsymbol{x}\|^2/t+\|\boldsymbol{v}\|^2 t$, we can force the term with the directional information $\boldsymbol{x}\cdot\boldsymbol{v}$ out of the integrals so that, when calculating the age, it is left out and the age field is provided by

$$a(\boldsymbol{x},t)=\frac{\int_0^t t'\Phi(\|\boldsymbol{x}\|,t')\mathrm{d}t'}{\int_0^t \Phi(\|\boldsymbol{x}\|,t')\mathrm{d}t'} \tag{3.11}$$

with

$$\Phi(\|\boldsymbol{x}\|,t')=\frac{Q(t-t')}{\sqrt{t'}^n}\exp\left[-\frac{\|\boldsymbol{x}\|^2}{t'}-\|\boldsymbol{v}\|^2 t'\right]\exp\left[-\gamma t'\right]. \tag{3.12}$$

Not surprisingly, since $\Phi\geq 0$, it is readily demonstrated that $a\leq t$. On the other hand, we see that for a point release, the age field is isotropic around the release point, regardless of the flow's direction and the particular form of the release $Q(t)$.

Another way of establishing that the age field is symmetric for a point release without making use of the age concentration field α is to observe that

$$C=\exp[2\boldsymbol{x}\cdot\boldsymbol{v}]F(r,t) \tag{3.13}$$

with $r=\|\boldsymbol{x}\|$. But then the "effective" advection in the age equation (2.8) is purely radial:

$$\boldsymbol{v}-\frac{\boldsymbol{\nabla}C}{2C}=\frac{1}{F}\frac{\partial F}{\partial r}\boldsymbol{e}_r, \tag{3.14}$$

where $\boldsymbol{e}_r$ is the radial unit vector. This means that for a zero initial age, since the effective advection is always radial and the diffusion isotropic, the point source will always lead to a symmetric and isotropic age field. This holds even if instead of imposing a zero age-concentration of the source, one imposes a given age on $\|\boldsymbol{x}\|=R$, for example. Though the age field will be different in this case, it will still be symmetric.

One may wonder whether the particular symmetry effect in the age field arises from the definition of the age via the concentration distribution function and if other definitions could lead to asymmetric age fields. Traditionally, rather than calculating

the age by the previous method, diagnoses may be carried out on radioactive tracers and the ratios of two different tracers. This is the way radiocarbon dating is performed in the ocean. To see whether such an approach modifies the symmetric nature of the radio-age field, we assume that we have two radioactive tracers C_1 and C_2 with the same input function but with different decay rates γ_1 and γ_2. The ratio of the two concentrations is thus

$$\frac{C_1(\boldsymbol{x},t)}{C_2(\boldsymbol{x},t)} = \frac{\int_{R^n}\int_0^t \frac{q(\boldsymbol{x}',t')}{\sqrt{\pi(t-t')}^n}\exp\left[\frac{-\{\boldsymbol{x}-\boldsymbol{x}'-\boldsymbol{v}(t-t')\}^2}{t-t'} - \gamma_1(t-t')\right]\mathrm{d}t'\mathrm{d}\boldsymbol{x}'}{\int_{R^n}\int_0^t \frac{q(\boldsymbol{x}',t')}{\sqrt{\pi(t-t')}^n}\exp\left[\frac{-\{\boldsymbol{x}-\boldsymbol{x}'-\boldsymbol{v}(t-t')\}^2}{t-t'} - \gamma_2(t-t')\right]\mathrm{d}t'\mathrm{d}\boldsymbol{x}'}. \tag{3.15}$$

Here the directional information cancels out for a point release, exactly as for a. Therefore, any age calculation based on radioactive decay rates like

$$a_r = -\frac{1}{\gamma_1-\gamma_2}\log\left(\frac{C_1}{C_2}\right) \tag{3.16}$$

will have the same symmetry properties as the age defined by α/C. In particular, the age defined by (3.16) around a local source is also isotropic.

3.1.1. Asymptotic behaviors. Though formally the solutions for the point release are given by integrals (3.9) and (3.10), their behavior is not straightforward to analyze. If we assume a constant source $Q(t) = q$, both integrals are of the following type (up to a multiplicative factor):

$$I(\rho,t) = \int_0^t \theta^\nu \exp\left[-\left(\frac{\rho^2}{\theta} - (1+\gamma)\theta\right)\right]\mathrm{d}\theta. \tag{3.17}$$

This integral has no closed analytical form, but we can obtain information regarding the behavior of this integral (and thus the concentration and age) by using asympotic expansions for large t or small t.

For $t^2 \ll \rho^2(1+\gamma)^{-1}$ the integral can be approximated by

$$I(\rho,t) \sim \int_0^t \theta^\nu \exp\left[-\frac{\rho^2}{\theta}\right]d\theta = (\rho^2)^{1+\nu}\Gamma[-1-\nu,\rho^2 t^{-1}], \tag{3.18}$$

where the incomplete Gamma function Γ can also be replaced by its asymptotic behavior for very large ρ^2/t, in which case

$$I(\rho,t) \sim \frac{t^{2+\nu}}{\rho^2}\exp\left[-\frac{\rho^2}{t}\right]. \tag{3.19}$$

Using this development in (3.9) and (3.10), it appears that, be it in one, two, or three dimensions, the age field for the initial moments near the origin behaves, as one might expect, like $a \sim t$.

For large t one can rewrite the integral I as

$$I = \int_0^\infty \theta^\nu \exp\left[-\frac{\rho^2}{\theta} - (1+\gamma)\theta\right]\mathrm{d}\theta - \int_t^\infty \theta^\nu \exp\left[-\frac{\rho^2}{\theta} - (1+\gamma)\theta\right]\mathrm{d}\theta. \tag{3.20}$$

The first integral is tabulated in [14] in terms of modified Bessel functions K_n, while in the second integral we assume $\rho^2(1+\gamma)^{-1} \ll t^2$, so that one has

$$I(\rho,t) \sim I_1(\rho) - \int_t^\infty \theta^\nu \exp\left[-(1+\gamma)\theta\right]\mathrm{d}\theta, \tag{3.21}$$

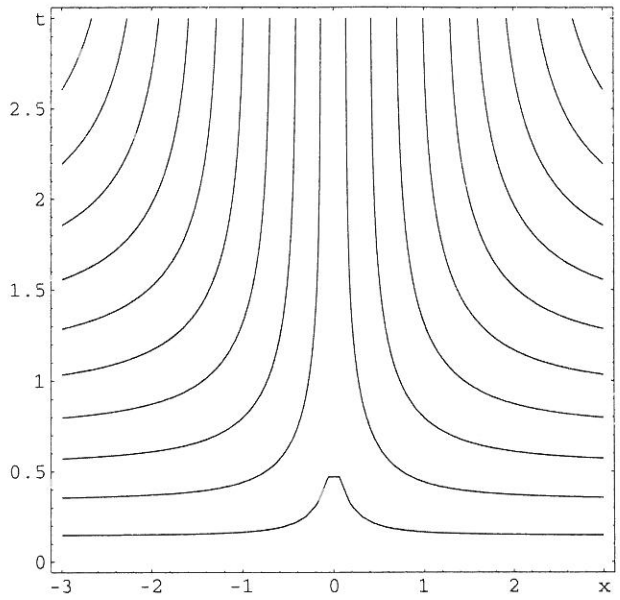

FIG. 2. *Age field for the* 1D *case in function of* x *and* t*; isolines start with small values for* $t = 0$ *and increase toward higher values of* t *with intervals of* 0.2.

$$I_1(\rho) = \frac{2}{(1+\gamma)^{1+\nu}} \left[(1+\gamma)\rho^2\right]^{\frac{1+\nu}{2}} K_{1+\nu}\left(2\sqrt{(1+\gamma)\rho^2}\right). \tag{3.22}$$

We can again develop the incomplete Gamma function, so that for large t

$$I(\rho, t) \sim I_1(\rho) - (1+\gamma)^{-1} t^{\nu} \exp[-(1+\gamma)t]. \tag{3.23}$$

In particular, for the 1D case, for small t we obtain

$$C \sim e^{2x} \frac{qt^{(3/2)}}{\sqrt{\pi}x^2} \exp\left[-\frac{x^2}{t}\right], \quad a \sim e^{2x} \frac{qt^{(5/2)}}{\sqrt{\pi}x^2} \exp\left[-\frac{x^2}{t}\right], \tag{3.24}$$

$$a \sim t. \tag{3.25}$$

For very large t age behaves then like

$$a \sim \frac{1+2|x|\sqrt{1+\gamma}}{2(1+\gamma)} \left[1 - \frac{1}{\sqrt{\pi t}} e^{-(1+\gamma)t+2\sqrt{(1+\gamma)x^2}} \left(1 - \frac{2t(1+\gamma)}{1+2|x|\sqrt{1+\gamma}}\right)\right]. \tag{3.26}$$

From Figure 2, it appears that the steady state is rapidly reached once $t \gg |x|$. This can be explained by the fact that the dominant contribution to the integrals is found near $t \sim x$ so that for $t \gg \|x\|$, the major contributions to the integrals are taken into account and the transient phase has occurred.

3.2. Nonpoint sources. In two dimensions, the symmetry in upwind and downwind directions remains if the sources are on a line perpendicular to the flow direction, and in three dimensions if the sources are on a plane perpendicular to the flow direction with central symmetries: In this case, q is independent of the coordinate x_v

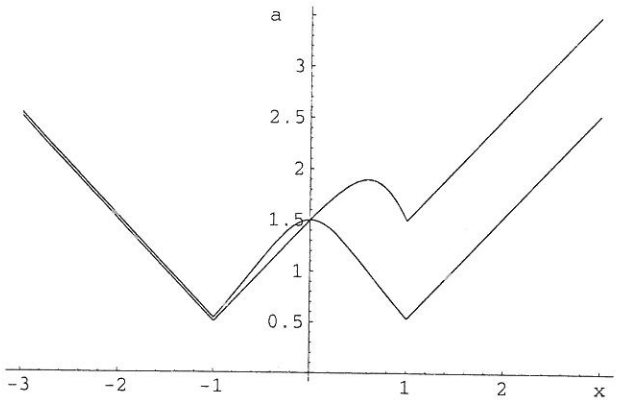

FIG. 3. *Age field for the* 1D *case in function of* x. *Symmetric source (upper curve) and downwind source* $q^+ = q^- \exp[4l]$ *(lower curve).*

along v, so that $\boldsymbol{x} = \boldsymbol{X} + x_v \boldsymbol{e}_v$, $\boldsymbol{e}_v \cdot \boldsymbol{v} = 1$, $\boldsymbol{X} \cdot \boldsymbol{e}_v = 0$ and the integrals involved again simplify out the terms in $\exp[2x_v]$

On the other hand, if the source term varies along the coordinate of the velocity direction, the symmetry of the age field can be destroyed. Indeed, consider the combination of two point sources along the current disposed symmetrically at $x = \pm l$ with intensity q^+ and q^-. The stationary solution (for $\gamma = 0$) reads

(3.27)
$$a = \frac{q^+(|x-l|+1/2)\exp[2(x-l-|x-l|)] + q^-(|x+l|+1/2)\exp[2(x+l-|x+l|)]}{q^+\exp[2(x-l-|x-l|)] + q^-\exp[2(x+l-|x+l|)]}.$$

This solution is depicted in Figure 3 for identical sources and an asymmetric source $q^+ = q^- \exp[4l]$.

For a symmetric source ($q^+ = q^-$), the age is greater in the downstream direction ($x > 0$), since older tracers (originating from the source q^-) have been advected from the upwind direction and add to the age of the tracer mix. When $q^+ = q^- \exp[4l]$, inspection of (3.27) shows that $a(x) = a(-x)$. A symmetric age field is obtained because the downwind source q^+ now adds a sufficient number of new tracers.

It is readily shown from the general solutions for C and α that, in general, the age is symmetric if the source distribution satisfies

(3.28)
$$q(x,t) = q(-x,t)e^{4x}.$$

4. Stationary solutions. The asymptotic developments of the preceding section can be used to write down explicitly the stationary solutions (Table 1) of a constant point release in one, two, and three dimensions by calculating the integrals (3.9) and (3.10) for $t \to \infty$.

It is possible to verify that integration of 3D to 2D to 1D is compatible for sources regardless of the corresponding direction.

Here, we show the solutions in the case of a 2D situation. As expected, the tracer field is advected downstream with a lateral and upstream diffusion (Figure 4).

TABLE 1
Stationary values for the point release in one, two, and three dimensions.

	C	α	a
1D	$\frac{q}{\sqrt{1+\gamma}} e^{[2x-2\sqrt{1+\gamma}\lvert x\rvert]}$	$\frac{q}{\sqrt{1+\gamma}^3} \frac{1+2\sqrt{1+\gamma}\lvert x\rvert}{2} e^{[2x-2\sqrt{1+\gamma}\lvert x\rvert]}$	$\frac{1+2\lvert x\rvert\sqrt{1+\gamma}}{2(1+\gamma)}$
2D	$\frac{q}{\pi} e^{[2\boldsymbol{x}\cdot\ \boldsymbol{v}]} 2K_0\left(2\sqrt{1+\gamma}\lVert\boldsymbol{x}\rVert\right)$	$\frac{q}{\pi} e^{[2\boldsymbol{x}\cdot\ \boldsymbol{v}]} \frac{2}{\sqrt{1+\gamma}} \lVert\boldsymbol{x}\rVert K_1\left(2\sqrt{1+\gamma}\lVert\boldsymbol{x}\rVert\right)$	$\frac{\lVert\boldsymbol{x}\rVert}{\sqrt{1+\gamma}} \frac{K_1(2\sqrt{1+\gamma}\lVert\boldsymbol{x}\rVert)}{K_0(2\sqrt{1+\gamma}\lVert\boldsymbol{x}\rVert)}$
3D	$\frac{q}{\pi} e^{[2\boldsymbol{x}\cdot\ \boldsymbol{v}]} \frac{1}{\lVert\boldsymbol{x}\rVert} e^{[-2\sqrt{1+\gamma}\lVert\boldsymbol{x}\rVert]}$	$\frac{q}{\pi} e^{[2\boldsymbol{x}\cdot\ \boldsymbol{v}]} \frac{1}{\sqrt{1+\gamma}} e^{[-2\sqrt{1+\gamma}\lVert\boldsymbol{x}\rVert]}$	$\frac{\lVert\boldsymbol{x}\rVert}{\sqrt{1+\gamma}}$

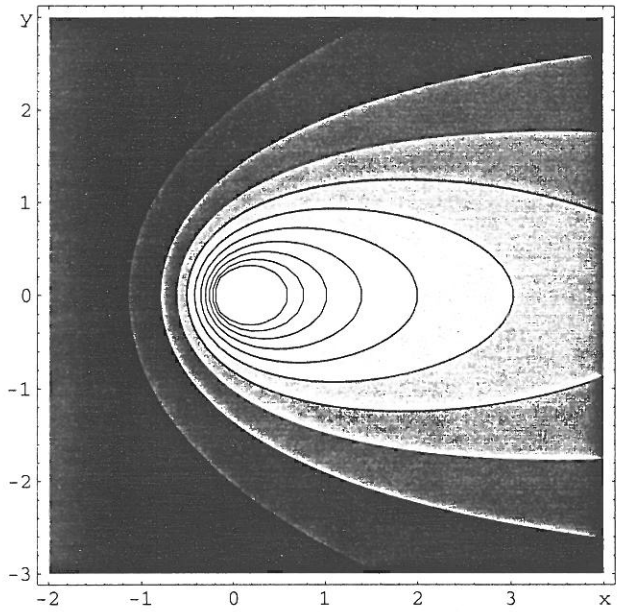

FIG. 4. *Tracer concentration field C in two dimensions around the release point $(0,0)$, with advection to the right. Low values are black and high values white.*

Similarly, the age-concentration field is influenced by advection (Figure 5), whereas the age field exhibits isotropic behavior (Figure 6), ignoring all directional information of the flow.

The same behavior can be observed in one and three dimensions, albeit with differences in the behavior of the fields close to the origin: the tracer concentration has a finite value at the origin in one dimension, a logarithmic singularity in two dimensions, and a simple pole singularity in three dimensions. The age field also behaves differently near the origin (Figure 7), with the greatest age in one dimension. It can be noticed that in all cases the asymptotic behavior for distant points is $a \sim \|\boldsymbol{x}\|/\sqrt{1+\gamma}$. In the absence of decay ($\gamma = 0$), in dimensional variables, age behaves like $\|\boldsymbol{x}\|/\|\boldsymbol{u}\|$, which is the advective age. Surprisingly, this age is also found in the upwind direction.

5. Time-varying current field. So far, we assumed $\boldsymbol{v}$ to be a constant velocity field, but some results can be extended to a time-varying velocity field. The general solution of the problem can be calculated as before by defining

$$\boldsymbol{v}(t) = \frac{\boldsymbol{u}(t)}{U}, \tag{5.1}$$

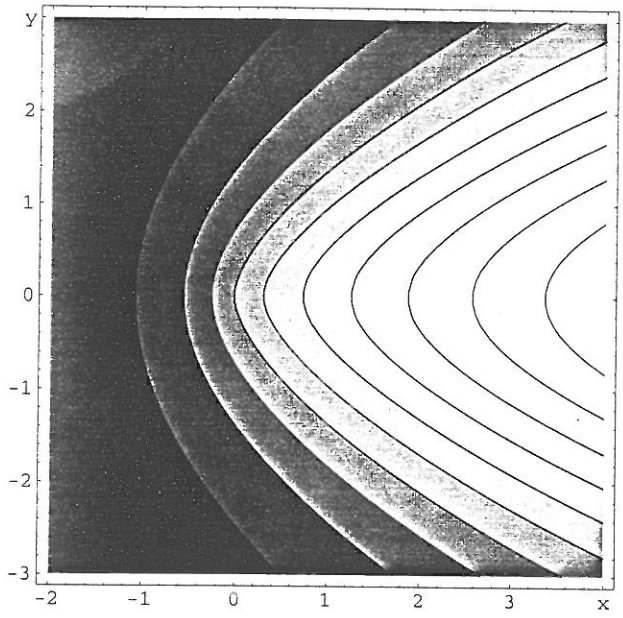

FIG. 5. *Age concentration field α around the release point.*

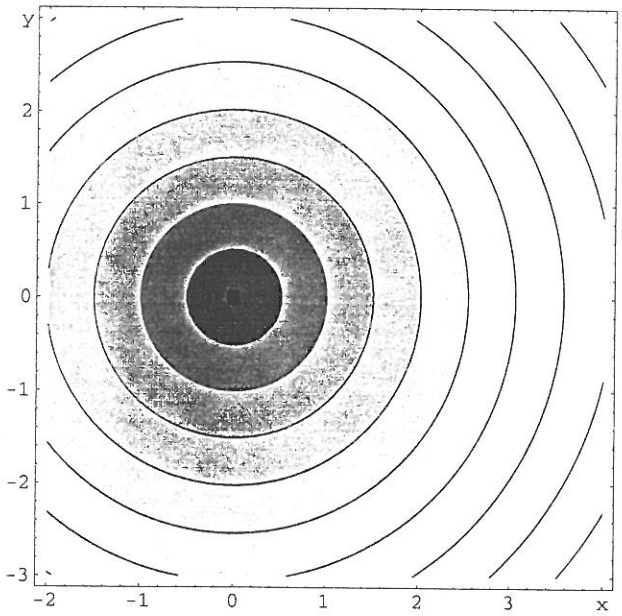

FIG. 6. *Age field around the release point.*

where U is the typical intensity of the current. By defining in addition

$$\boldsymbol{w}(t,t_0) = \frac{1}{t-t_0}\int_{t_0}^{t} \boldsymbol{v}(t')\mathrm{d}t' \tag{5.2}$$

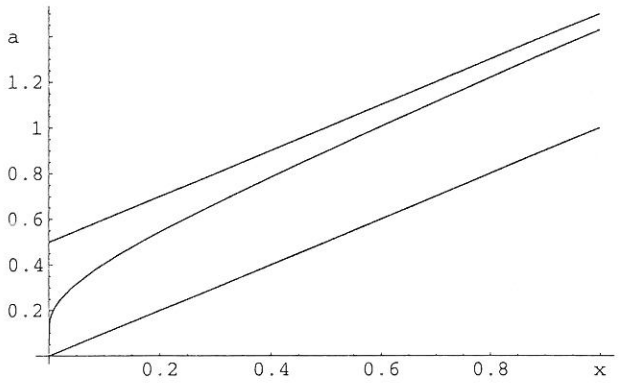

FIG. 7. *Stationary age a depending on the nondimensional distance to the release point for the* 1D *(upper curve),* 2D *(middle), and* 3D *(lower curve) cases.* $\gamma = 0$.

the fundamental solutions for a Dirac release in space and time $t = t_0$ read

$$C(\boldsymbol{x}, t, t_0) = \frac{q}{\sqrt{\pi(t-t_0)}^n} \exp\left[\frac{-\big(\boldsymbol{x} - \boldsymbol{w}(t,t_0)(t-t_0)\big)^2}{t-t_0}\right] \exp\left(-\gamma(t-t_0)\right), \tag{5.3}$$

$$\alpha(\boldsymbol{x}, t, t_0) = (t-t_0)\frac{q}{\sqrt{\pi(t-t_0)}^n} \exp\left[\frac{-\big(\boldsymbol{x} - \boldsymbol{w}(t,t_0)(t-t_0)\big)^2}{t-t_0}\right] \exp\left(-\gamma(t-t_0)\right), \tag{5.4}$$

and the general solution for arbitrary releases can again be obtained by convolution integrals.

Now the term in $\exp[\boldsymbol{x}\cdot\, \boldsymbol{w}]$ cannot be forced out of the integral because of the dependence of $\boldsymbol{w}$ on time. This leads to the possibility of having an asymmetric age field in a time-varying current field. To see the possible strength of this asymmetry, we will look at the function $S = a(\boldsymbol{x})a(-\boldsymbol{x})^{-1}$:

$$S = \frac{\int_0^t t'\Phi(\|\boldsymbol{x}\|, t') \exp[2\boldsymbol{x}\cdot\, \boldsymbol{w}(t, t-t')]\mathrm{d}t' \int_0^t \Phi(\|\boldsymbol{x}\|, t'') \exp[-2\boldsymbol{x}\cdot\, \boldsymbol{w}(t, t-t'')]\mathrm{d}t''}{\int_0^t t'\Phi(\|\boldsymbol{x}\|, t') \exp[-2\boldsymbol{x}\cdot\, \boldsymbol{w}(t, t-t')]\mathrm{d}t' \int_0^t \Phi(\|\boldsymbol{x}\|, t'') \exp[2\boldsymbol{x}\cdot\, \boldsymbol{w}(t, t-t'')]\mathrm{d}t''} \tag{5.5}$$

with

$$\Phi(\|\boldsymbol{x}\|, t') = \frac{Q(t-t')}{\sqrt{\pi t'}^n} \exp\left[-\frac{\|\boldsymbol{x}\|^2}{t'} - \|\boldsymbol{w}\|^2 t'\right] \exp\left[-\gamma t'\right]. \tag{5.6}$$

It is clear that

$$\begin{aligned} &\exp[\min\big(4\boldsymbol{x}\cdot\, \{\boldsymbol{w}(t, t-t') - \boldsymbol{w}(t, t-t'')\}\big)] \le S \\ &\le \exp[\max\big(4\boldsymbol{x}\cdot\, \{\boldsymbol{w}(t, t-t') - \boldsymbol{w}(t, t-t'')\}\big)], \end{aligned} \tag{5.7}$$

where the min and max values are computed for all couples of t' and t''. This means that for a given maximum, there is always a minimum which is the maximum with changed sign (and vice versa), so that if b denotes the positive maximum, we obtain

$$\exp[-b] \le S \le \exp[b], \tag{5.8}$$

$$b = \max\left(|4\boldsymbol{x}\cdot\{\boldsymbol{w}(t,t-t') - \boldsymbol{w}(t,t-t'')\}|\right). \tag{5.9}$$

For very small b, the age is thus symmetric, since $S \sim 1$, which is the case if $|\boldsymbol{x}\cdot\delta\boldsymbol{w}| \ll 1$, with $\delta\boldsymbol{w}$ being a typical variation of the vector $\boldsymbol{w}$.

The symmetry may, however, extend beyond this distance. Indeed, the major contributions to the integrals are all found near the points $t' \sim \|\boldsymbol{x}\|/\|\boldsymbol{w}\|$, but near these points, the asymmetric contribution $\boldsymbol{w}(t,t-t') - \boldsymbol{w}(t,t-t'')$ is much smaller than the estimated upper bounds, since $t' \sim t''$ if $\|\delta\boldsymbol{w}\| \ll \|\boldsymbol{w}\| \sim 1$.

We can also mention that there is no reason for asymmetry in a specific direction since it depends on the way $\boldsymbol{w}$ varies.

For large t', $\boldsymbol{w}(t,t-t') \to 1$ (if scaling was performed appropriately). This means that if the contribution to the integral is predominantly found in the higher values of t', the solution will be symmetric: due to $\boldsymbol{w}$ being almost constant in this scenario, its contribution cancels out. Since the integrand is maximum near the points where $t' \sim \|\boldsymbol{x}\|$, for large t and points far away, the solution will also tend to be symmetric.

To further analyze the problem, we focus now on a system illustrative of a tidal current u_1 superimposed on a residual current u_0. Such a situation is typical for coastal systems. In such cases one might ask whether a local release of radioactive tracers at the coast (near a nuclear waste treatment plant, for example) also leads to a symmetric age field or if the tidal motion induces asymmetry. In nondimensional form ($v_1 = u_1/u_0$), $v = 1 + v_1\cos(\omega t)$, so that

$$w(t,t-t') = 1 + v_1\frac{2\sin\left(\frac{\omega t'}{2}\right)}{\omega t'}\cos\left(\omega t - \frac{\omega t'}{2}\right). \tag{5.10}$$

In view of the function $\sin x/x$, we can estimate $b \sim 4.8 v_1 x$, so that for $|x| \ll \frac{1}{5v_1}$ the solution will be symmetric.

For the tidal system with a residual current, $\boldsymbol{w}$ will tend to a stationary value for $t' \gg t^l$ several times the period of the tide, multiplied by the magnitude of the tidal current:

$$t^l \sim \frac{v_1}{\omega}. \tag{5.11}$$

But for $t, t' \gg t^l$ and for distant points, the main contribution to the integrals is near $\|\boldsymbol{x}\| \sim t$, so that for $\|\boldsymbol{x}\| \gg \frac{v_1}{\omega}$ and for large t, the main contributions to the integrals are found around $\boldsymbol{w} \sim 1$ and the age will be symmetric. In terms of physical variables this implies that for points several tidal excursions away, the stationary solution will be symmetric. But since the solution is also symmetric if $\|\boldsymbol{x}\| \ll v_1^{-1}$, a necessary condition for the existence of asymmetry is that

$$v_1^2 \not\ll \omega. \tag{5.12}$$

To analyze this problem in more detail, we have to look more exactly where an integrand of the form

$$t^\nu \exp[-\|\boldsymbol{x}\|^2/t - \|\boldsymbol{w}\|t] \tag{5.13}$$

provides the maximum contribution to the integral: This happens around

$$t^* = \frac{\nu + \sqrt{\nu^2 + 4\|\boldsymbol{x}\|^2\|\boldsymbol{w}\|^2}}{2\|\boldsymbol{w}\|^2} \tag{5.14}$$

if we assume that w is dominated by its locally constant part.

The asymmetry can only be present because the value of ν is different for the integrals involved. By looking at the definition of S, we see that we are in the presence of integrals in $\nu = -n/2$ and $\nu = -n/2 + 1$. If the contribution to the integral in $-n/2$ is near t_1, then the maximum contribution to the second integral is near $t_2 = t_1 + \|w\|^{-2}/2$. The more w has changed between these two moments, the stronger we expect the asymmetry to be. In other words, for an oscillating current whose period is $2(t_2 - t_1)$

$$\omega^* = 2\|w\|^2\pi \tag{5.15}$$

an asymmetry will probably occur. Moreover, the asymmetry will be stronger if the contribution to the integrals is near the first oscillations of w in function of t', because for $t \gg t^l$, the variations are too small. The strongest variations are found for

$$t' \sim \frac{\pi}{2\omega^*} \tag{5.16}$$

since significant changes still have to occur for w.

For $\omega \gg \omega^*$, w rapidly tends to 1 and for $t' \gg v_1/\omega$, the system tends to be symmetric for points $\|x\| \gg t^l$.

For $\omega \ll \omega^*$ the maximum contributions to the integrals take place for t' near t_1 and t_2 for which $|t_1 - t_2|\omega \ll 1$ so that the function w is almost constant between these two moments and the asymmetry very weak. This case may also be interpreted by observing that for small ω and $t \ll \omega^{-1}$, $w \sim 1 + v_1$, so that we are in a situation of a uniform current, simply because the current varies very slowly.

So we basically expect symmetry near the origin on a scale of $1/v_1$, far away for scales larger than the tidal excursion and t_l, while the strongest asymmetry is expected for $\omega^* \sim 2\pi$ near the tidal excursion point.

This behavior is depicted in Figure 8 for different values of v_1 and ω.

Finally, we can analyze the case for which $\epsilon = v_1\omega^{-1} \ll 1$. In this case,

$$w(t, t - t') = 1 + \epsilon\frac{F(t, t')}{t'}, \tag{5.17}$$

$$F(t, t') = 2\sin\left(\frac{\omega t'}{2}\right)\cos\left(\omega t - \frac{\omega t'}{2}\right) = O(1), \tag{5.18}$$

and we can develop exponential functions for small ϵ:

$$\begin{aligned} &\exp\left[\frac{-(x - w(t, t - t')t')^2}{t'}\right] \sim \exp\left[\frac{-(x - t')^2}{t'}\right]\exp\left[2\epsilon\frac{x - t'}{t'}F - \epsilon^2\frac{F^2}{t'}\right] \\ &\sim \exp\left[\frac{-(x - t')^2}{t'}\right]\left(1 + 2\epsilon\frac{x - t'}{t'}F - \epsilon^2\frac{F^2}{t'} + \frac{1}{2}\left[2\epsilon\frac{x - t'}{t'}F - \epsilon^2\frac{F^2}{t'}\right]^2\right). \end{aligned} \tag{5.19}$$

From here on it is clear that if we integrate the solution over a tidal cycle $T = \frac{2\pi}{\omega}$ by defining an average solution

$$\overline{C(x, t, t')} = \frac{1}{T}\int_t^{t+T} C(x, t, t')\mathrm{d}t, \tag{5.20}$$

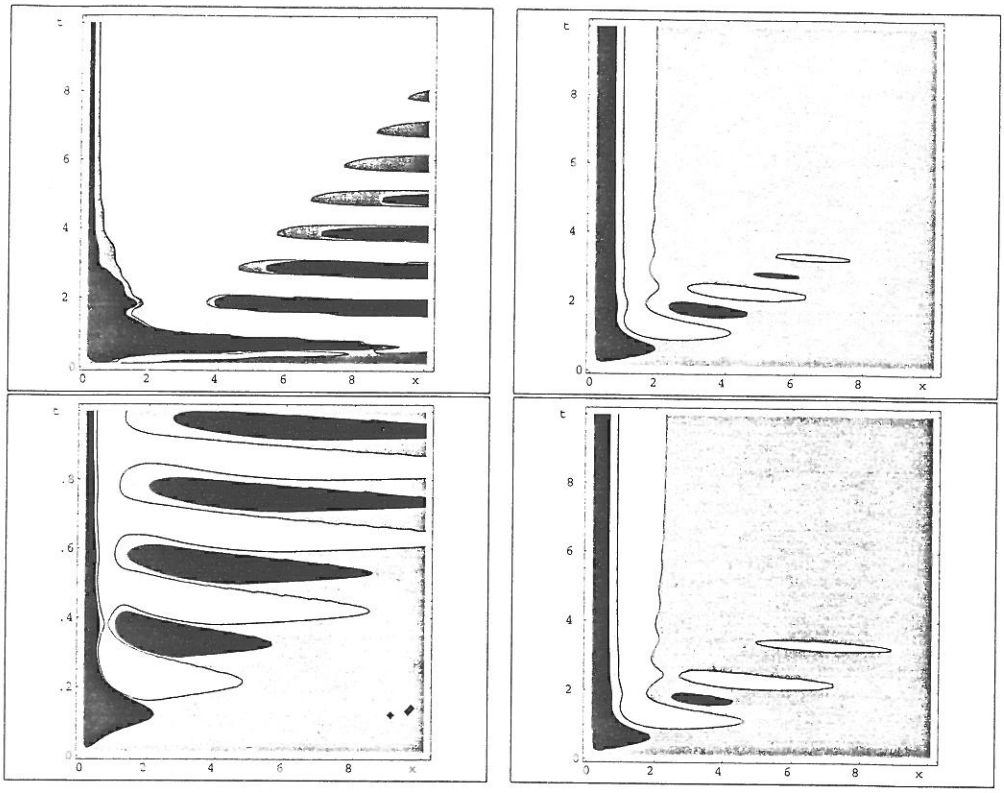

FIG. 8. *S for the* 1D *case in function of* (x,t). *Upper left:* $\omega = 2\pi, \upsilon = 1 + 10\cos(\omega t), \gamma = 0$. *Upper right:* $\omega = 2\pi, \upsilon = 1 + 0.1\cos(\omega t), \gamma = 0$. *Lower left:* $\omega = 10\pi, \upsilon = 1 + 10\cos(\omega t), \gamma = 0$. *Lower right:* $\omega = 2\pi, \upsilon = 1 + \cos(\omega t), \gamma = 0$ *Black indicates values below* 0.99 *and white above to* 1.01. *Gray corresponds thus to a symmetric situation at a* 1% *level.*

the contributions from odd power in ϵ disappear, because for odd powers of ϵ, F also appears as odd powers and the integrals

$$\frac{1}{T}\int_t^{t+T} \cos^{(2n+1)}(\omega t - \omega t'/2)\mathrm{d}t = 0, \quad \frac{1}{T}\int_t^{t+T} \cos^2(\omega t - \omega t'/2)\mathrm{d}t = 1/2. \tag{5.21}$$

So compared to the solution for $\epsilon = 0$, for the tidally averaged solution a multiplication factor appears of

$$1 + 2\sin^2\left(\frac{\omega t'}{2}\right)\frac{2(x-t')^2 - t'}{t'^2}\epsilon^2, \tag{5.22}$$

which shows that the asymmetry for the tidal average is highest in ϵ^2 rather than in ϵ.

6. Stationary solution for the concentration distribution function c. A particularly interesting case arises when one assumes a stationary solution in the temporal domain, i.e., $\frac{\partial}{\partial t} = 0$.

The stationary concentration distribution equation thus reads

$$\frac{\partial c}{\partial \tau} = p - d - \nabla\cdot\left(uc - \boldsymbol{K}\cdot\nabla c\right). \tag{6.1}$$

Formally, this is identical to the nonstationary advection-diffusion equation for a classical tracer. Since for numerical models, stationary solutions of time-dependent equations are often calculated by a time-marching procedure, we might wonder whether the formal equivalence of (2.1) could be used with a time-dependent problem. This would allow forward integration in the τ-space, providing the concentration distribution function and the stationary tracer concentration fields. This would indeed provide an insight into the age composition of the tracer field.

Since the stationary tracer concentration is simply

$$C(\boldsymbol{x}) = \int_0^\infty c(\boldsymbol{x}, \tau)\mathrm{d}\tau \tag{6.2}$$

the knowledge of the concentration distribution function is sufficient to calculate the tracer field which also obeys the classical equation

$$0 = P - D - \boldsymbol{\nabla}\cdot\left(uC - \boldsymbol{K}\cdot\boldsymbol{\nabla}C\right). \tag{6.3}$$

Once the concentration distribution c is known, the tracer field can be calculated by (6.2), while the tracer age a can be determined by

$$a(\boldsymbol{x}) = \frac{1}{C}\int_0^\infty \tau c(\boldsymbol{x}, \tau)\mathrm{d}\tau. \tag{6.4}$$

We would like to investigate the possibility of calculating the stationary concentration distribution function by using a standard "nonstationary" advection-diffusion solver. The question remains of how to define an "age"-dependent problem which allows us to calculate the original stationary tracer problem. Since the nonstationary tracer problem obeys the same kind of advection-diffusion equation as the same stationary concentration distribution functions we are looking for, we simply have to find appropriate source terms p and d, as well as initial and boundary conditions for the concentration distribution fields, which when applied give a solution allowing us to retrieve the stationary tracer distribution in accordance with the original problem.

If the stationary tracer C is subjected to time-independent external source and sink terms, as well as boundary conditions, these terms may be used to define the "age" at the boundaries and the inputs into the system.

Examples of boundary conditions follow:

For a point release in $\boldsymbol{x}_r$ with constant input Q for C, one imposes the age of the input to be μ. In this case,

$$P = Q\delta(\boldsymbol{x} - \boldsymbol{x}_r),\ p = Q\delta(\boldsymbol{x} - \boldsymbol{x}_r)\delta(\tau - \mu), \tag{6.5}$$

where δ is the classical Dirac function.

For a Dirichlet boundary condition on the boundary $\boldsymbol{x} = \boldsymbol{x}_b$

$$C(\boldsymbol{x}_b) = C^b(\boldsymbol{x}_b). \tag{6.6}$$

One can impose the age at that boundary to be $\mu^b(\boldsymbol{x}_b)$:

$$c(\boldsymbol{x}_b, \tau) = C^b(\boldsymbol{x}_b)\delta(\mu^b(\boldsymbol{x}_b) - \tau). \tag{6.7}$$

For general flux conditions in the tracer field (n being the normal direction to the boundary and a a time-independent coefficient)

$$\frac{\mathrm{d}C}{\mathrm{d}n} = aC + F(\boldsymbol{x}_b). \tag{6.8}$$

The choice of a boundary condition on the concentration distribution allows us to impose the "age" $\mu^b(\boldsymbol{x}_b)$ of the external flux F at this boundary:

$$\frac{\mathrm{d}c}{\mathrm{d}n} = ac + F(\boldsymbol{x}_b)\delta(\mu^b(\boldsymbol{x}_b) - \tau). \tag{6.9}$$

One could even decide not to impose a Dirac-like concentration distribution at the boundaries, using any normalized distribution instead. However, for practical purposes, one generally will look at systems where the age is prescribed as shown here.

The initial condition on the concentration distribution function defines the origin of the "age."

Practically, we can thus calculate the stationary concentration distribution function by solving a time-dependent problem (where "time" is in fact "age") with modified boundary conditions and source terms, during which the first-order moment can be diagnosed at each "moment" ("age"), which allows us to calculate the stationary tracer distribution as well as its age.

The concentration distribution function of the stationary problem is thus the Green function of a classical nonstationary problem for tracer dispersions.

From a practical point of view, the use of this method applied to a 3D numerical model allows us, by means of a single "time-" ("age-") dependent equation, to calculate the stationary tracer field, its concentration distribution function, its age, and the Green function of the stationary problem. The only modifications to the normal way the stationary solution is calculated are the adaptations of the boundary conditions and the necessity to integrate numerically the zeroth (6.2) and first-order moments (6.4) with respect to "time" during numerical integration.

This is, however, easily achieved, and from the same effort, we obtain additional insight into the physics of the problem and the way the diffusion-dispersion acts on the concentration distribution.

6.1. Example of stationary concentration distribution functions. Here we can use the solutions of the point release problem. Indeed, for the standard stationary tracer with a permanent release, we have just seen that we can first solve the nonstationary problem with a Dirac source instead of the permanent release. But the solution of this problem is simply the Green function (3.5).

In other words, the concentration distribution function for a permanent point release with zero age is

$$c(\boldsymbol{x},\tau) = C_g = \frac{Q}{\sqrt{\pi\tau}^n} \exp\left[\frac{-(\boldsymbol{x} - \boldsymbol{v}\tau)^2}{\tau}\right] \exp(-\gamma\tau). \tag{6.10}$$

Interestingly enough, this function can continue to be written as

$$c(\boldsymbol{x},\tau) = e^{2\boldsymbol{x}\cdot\boldsymbol{v}} \frac{Q}{\sqrt{\pi\tau}^n} \exp\left[\frac{-\|\boldsymbol{x}\|^2}{\tau} - \tau\right] \exp(-\gamma\tau) = e^{2\boldsymbol{x}\cdot\boldsymbol{v}} \Phi(\|\boldsymbol{x}\|,\tau), \tag{6.11}$$

so that the concentration distribution in function of τ has the same shape given by $\Phi(\|\boldsymbol{x}\|,\tau)$ around the release point. Only the amplitude of the distribution has changed nonisotropically (due to the factor $\exp(2\boldsymbol{x}\cdot\boldsymbol{v})$), so that all points with the same distance from the source have the same shape as the concentration distribution function regardless of the direction of the flow. For a given distance from the source, we thus always find the same proportions of older and newer components of the tracer mix (though the total amounts are of course higher in downwind directions).

To retrieve the stationary solution of the permanent release, one can use (6.2) or use the nonstationary solution of the classical constant release problem by using the convolution theorem with the Green function (thus adding up the individual contributions of a series of Dirac functions):

$$C(\boldsymbol{x},t) = \int_0^t C_g(\boldsymbol{x},t')Q(t-t')\mathrm{d}t'. \tag{6.12}$$

For a time-independent source term and for $t \to \infty$ we retrieve indeed (6.2), which was explicitly calculated in one, two, and three dimensions.

For the age field, one can calculate

$$a(\boldsymbol{x}) = \frac{1}{C}\int_0^\infty \tau C_g \mathrm{d}\tau, \tag{6.13}$$

and we retrieve the age fields already calculated.

7. Conclusions. The assessment of the age of a tracer or of a water mass is a powerful and highly flexible tool to diagnose complex flow fields. In numerical studies, tracers can be defined so as to match any specific need to assess specific time scales of the flow. We demonstrated, however, that counterintuitive results can emerge, such as the isotropy of the age field for a point release in a uniform flow field, regardless of the values of the diffusion and velocity or the discharge function.

Though asymmetric age fields can be generated by a time-varying current (as in a tidal system), the asymmetry is not systematic and no simple way of interpreting them was found.

Such results suggest therefore that a proper interpretation of age fields must always be carried out in parallel with the interpretation of the tracer field itself: the spatial distribution of the tracer concentration helps to identify the preferential directions of the flow while the age field allows to quantify the associated time scales.

We also presented a simple method by which a standard stationary tracer calculation can be extended so that its concentration distribution function and its age are assessed without having to solve additional differential equations. Simple modified boundary conditions and diagnostics allow us to solve both the initial problem of the stationary tracer field and its associated concentration distribution function and age. In the case of oceanographic applications, this could shed new light on simulations of deep water tracers, for example.

Acknowledgments. Two model intercomparisons were supported by the European Union (MEDMEX contract MAS2-CT94-0107, MATER contract MAS3-CT96-0051, NOMADS contract MAS2-CT94-0105 and MAS3-CT98-0163, and MEDNET contract MAS3-CT98-0189) and led to some questions addressed in the present paper.

REFERENCES

[1] ANONYMOUS, *Model Intercomparison, NOMADS (North Sea Model Advection-Dispersion Study)*, Technical report IV, Proudman Oceanographic Laboratory, Bidston Observatory, Birkenhead, Merseyside, UK, 1997.

[2] P. BECKER AND G. BJORK, *Residence times in the upper Arctic Ocean*, Journal of Geophysical Research, 101 (1996), pp. 28377–28396.

[3] P. BEINING AND W. ROETHER, *Temporal evolution of CFC11 and CFC12 concentrations in the ocean interior*, Journal of Geophysical Research, 101 (1996), pp. 16455–16464.

[4] M. BRETON AND J. C. SALOMON, *A 2D long term advection-dispersion model for the Channel and southern North Sea, Part A: Validation through comparison with artificial radionuclides*, Journal of Marine Systems, 6 (1995), pp. 495–513.

[5] W. Broecker, A. Virgilio, and T.-H. Peng, *Radiocarbon age of waters in the deep Atlantic revisited*, Geophysical Research Letters, 18 (1991), pp. 1–3.
[6] J.-M. Campin, T. Fichefet, and J. Duplessy, *Problems with using radiocarbon to infer ocean ventilation rates for past and present climates*, Earth and Planetary Science Letters, 165 (1999), pp. 17–24.
[7] E. Deleersnijder, J.-M. Campin, and E. Delhez, *The concept of age in marine modelling: Theory and preliminary model results*, Journal of Marine Systems.
[8] E. Deleersnijder, B. Tartinville, and J. Rancher, *A simple model of the tracer flux from the Mururoa lagoon to the Pacific*, Appl. Math. Lett., 10 (1997), pp. 13–17.
[9] E. Delhez, *Macroscale ecohydrodynamic modeling in the northwest European continental shelf*, Journal of Marine Systems, 16 (1998), pp. 171–190.
[10] E. Delhez, J.-M. Campin, A. Hirst, and E. Deleersnijder, *Toward a general theory of the age in ocean modelling*, Ocean Modelling, 1 (1999), pp. 17–27.
[11] E. Delhez and G. Carabin, *Integrated modelling of the Belgian coastal zone*, Estuarine Coastal and Shelf Science, accepted.
[12] S. Doney, W. Jenkins, and J. Bullister, *A comparison of ocean tracer dating techniques on a meridional section in the eastern North Altantic*, Deep Sea Research, 44 (1997), pp. 603–626.
[13] M. England, *The age of water and ventilation timescales in a global ocean model*, Journal of Physical Oceanography, 25 (1995), pp. 2756–2777.
[14] I. Gradshteyn and I. Ryzhik, *Table of Integrals, Series and Products*, Academic Press, New York, 1965.
[15] D. Haidvogel and F. Bryan, *Ocean General Circulation Modeling*, Cambridge University Press, Cambridge, UK, 1992, pp. 371–412.
[16] A. Hirst, *Determination of water component age in ocean models: Application to the fate of North Atlantic deep water*, Ocean Modelling, 1 (2000), pp. 81–94.
[17] W. Jenkins, *Studying subtropical thermocline ventilation and circulation using tritium and $_3He$*, Journal of Geophysical Research, 103 (1998), pp. 15817–15831.
[18] W. Jenkins and W. Clarke, *The distribution of $_3He$ in the western Atlantic Ocean*, Deep Sea Research, 23 (1976), pp. 481–494.
[19] J. Karstensen and M. Tomczak, *Age determination of mixed water masses using CFC and oxygen data*, Journal of Geophysical Research, 103 (1998), pp. 18599–18609.
[20] G. Ostlund, *Isotope tracing of Siberian river water in the Arctic Ocean*, Journal of Environmental Radioactivity, 25, pp. 57–63.
[21] R. Pickart, N. Hogg, and W. Smethie, Jr., *Determining the strength of the deep western boundary current using the chlorofluoromethane ratio*, Journal of Physical Oceanography, 19 (1989), pp. 940–951.
[22] D. Prandle, *A modeling study of the mixing of ^{137}Cs in the seas of the European Continental Shelf*, Philos. Trans. Roy. Soc. London A, 310 (1984), pp. 407–436.
[23] J.-C. Salomon, M. Breton, and P. Guegueniat, *A 2D long term advection-dispersion model for the Channel and southern North sea—Part B: Transit time and transfer function from Cap de La Hague*, Journal of Marine Systems, 6 (1995), pp. 515–527.
[24] P. Schlosser, *Mid-1980s distribution of tritium, $_3He$, ^{14}C and ^{39}Ar in the Greenland/Norwegian Seas and the Nansen Basin of the Arctic Ocean*, Progress in Oceanography, 35 (1995), pp. 1–28.
[25] M. Stuiver, P. Quay, and H. Ostlund, *Abyssal water carbon-14 distribution and the age of the world oceans*, Science, 219 (1983), pp. 849–851.
[26] H. Takeoka, *Fundamental concepts of exchange and transport time scales in a coastal sea*, Continental Shelf Research, 3 (1984), pp. 311–326.
[27] G. Thiele and J. Sarmiento, *Tracer dating and ocean ventilation*, Journal of Geophysical Research, 95 (1990), pp. 9377–9391.
[28] K. Turekian, N. Tanaka, V. Turekiann, T. Togersenn, and E. Deangelo, *Transfer rates of dissolved tracers through estuaries based on $_{228}Ra$: A study of Long Island Sound*, Continental Shelf Research, 16 (1996), pp. 863–873.
[29] D. Wallace, P. Schlosser, M. Krysell, and G. Bonish, *Halocarbon ratio and tritium/$_3He$ dating of water masses in the Nansen Basin, Arctic Ocean*, Deep Sea Research, 39 (1992), pp. 435–458.
[30] J. Zimmerman, *Mixing and flushing of tidal embayments in the western Dutch Wadden Sea—Part I: Distribution of salinity and calculation of mixing time scales*, Netherlands Journal of Sea Research, 10 (1976), pp. 149–191.